Phys. Chem. Earth, Vol. 17, pp. 1–9, 1989
Printed in Great Britain.

0079–1946/89 $0.00 + 0.50

Textural Development of Clayey and Quartzofeldspathic Fault Gouges Relative to their Sliding Behavior

D. E. MOORE and J. D. BYERLEE

U.S. Geological Survey, Menlo Park, CA 94025, U.S.A.

ABSTRACT

Many of the secondary fault structures developed during triaxial friction experiments have been generally correlated with the structures of natural fault zones. Therefore, any physical differences that can be found between laboratory samples that slide stably and those that show stick-slip motion may help to identify the cause of earthquakes. We have examined petrographically the run products of many triaxial friction experiments using clayey and quartzofeldspathic gouges, which comprise the principal types of natural fault gouge material. The examined samples were tested under a wide range of temperature, confining and fluid pressure, and velocity conditions.

The clayey and quartzofeldspathic gouges show some textural differences, owing to their different mineral contents and grain sizes and shapes. In the clayey gouges, for example, a clay mineral fabric and kink band sets are commonly developed, whereas in the quartzofeldspathic gouges fracturing and crushing of the predominately quartz and feldspar grains are important processes. For both types of gouge, however, and whatever the pressure-temperature-velocity conditions of the experiments, the transition from stable sliding to stick-slip motion is correlated with: (i) a change from pervasive deformation of the gouge layer to localized slip in subsidiary shears; and (ii) an increase in the angle between the shears that crosscut the gouge layer (Riedel shears) and ones that form along the gouge-rock cylinder boundaries (boundary shears). This suggests that the localization of shear within a fault zone combined with relatively high Riedel-shear angles are somehow connected with earthquakes.

Secondary fracture sets similar to Riedel shears have been identified at various scales in major strike-slip faults such as the San Andreas of the western United States (Wallace, 1973) and the Luhuo and Fuyun earthquake faults of China (Deng and Zhang, 1984; Deng *et al.*, 1986). The San Andreas also contains locked and creeping sections that correspond to the stick-slip and stably sliding experimental samples, respectively. We plan to study the physical structure of the San Andreas fault, to see if the experimentally observed differences related to sliding behavior can also be distinguished in the field.

INTRODUCTION

For the past several years, we have measured the frictional properties of a number of different fault gouge materials under varying conditions of temperature, confining pressure, fluid pressure, and strain rate. The samples tested during the friction experiments either slide stably or show the stick-slip type of motion that is considered to be the laboratory equivalent of earthquakes (e.g. Fig. 1). We recently began a

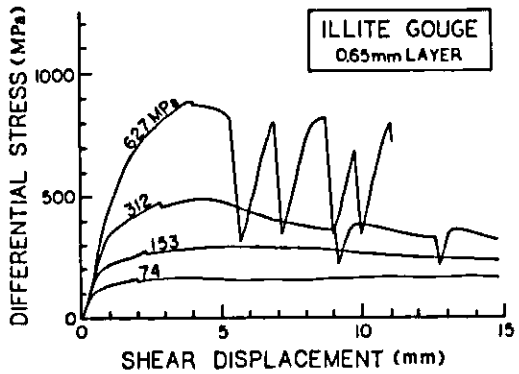

Fig. 1. Plot of differential stress versus shear displacement along the sawcut for samples of illite gouge run dry at room temperature, at a strain rate of 10^{-4}/s. Increasing the confining pressure from 74 to 627 MPa leads to an increase in strength of the gouge and a change from stable to stick-slip motion.

petrographic study of the run products of the friction experiments, to see if there are any physical differences between the samples that slide stably and those that show stick-slip motion. Many of the structures developed during triaxial experiments and Riedel and shear box tests can be correlated with the structures of natural fault zones (Tchalenko, 1970). Therefore, any physical differences that can be found between the stably sliding and stick-slip samples may help to explain natural earthquake processes. This paper compares the deformation textures developed during stable and stick-slip motion in clay-rich and quartzofeldspathic gouges, and describes how the results will be tested against fault zones.

ILLITE GOUGE

The clayey gouge that was examined in detail is a disaggregated illitic shale from Fithian, Illinois. The gouge contains about 70% illite, 20% quartz, and 10% kaolinite plus chlorite (Moore *et al.*, 1983), along with trace amounts of opaque and calcite grains. The experimental samples consisted of a layer of gouge 0.65 mm in initial thickness that was placed along a 30° sawcut surface in a granite cylinder. The experiments were run at temperatures up to 600°C, strain rates of 10^{-4}/s to 10^{-6}/s, and a variety of confining and pore pressures. Selected strength data at room temperature and at elevated temperatures are shown in Figs 1 and 2, respectively, and the rest are contained in Summers and Byerlee (1977) and in Moore *et al.* (1986a). The illite-rich gouge shows increases in strength and a change from stable to stick-slip motion with increasing effective pressure (Fig. 1) and increasing temperature (Fig. 2). At a given set of pressure-temperature conditions, stick-slip is more common and the stress drops tend to be larger in the experiments at the slower strain rate (Fig. 2).

Photomicrographs showing the range of textures developed in the illite gouge run products are presented in Fig. 3. Some of the samples are pervasively deformed (Fig. 3a), and the textures include a clay-mineral alignment, stretched mineral grains, an array of low-angle kink bands, and high-angle kink/fold structures. In the samples characterized by Fig. 3b, the low-angle kink bands have a more restricted occurrence: Individual bands do not cross the entire gouge layer, rather, they occur as short segments that are grouped together along the gouge-rock cylinder boundaries and in narrow zones that cross the gouge layer at a somewhat lower angle than the kink band orientations. These zones of low-angle kinks appear to represent proto-shear zones within the gouge layer.

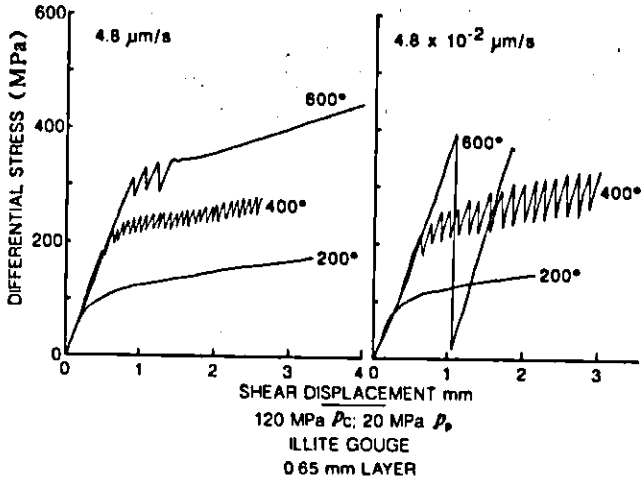

Fig. 2. Strength data for heated illite gouge at 100MPa effective pressure and sliding velocities of 4.8 and 4.8 × 10^{-2} μm/s along the sawcut, which correspond to strain rates of 10^{-4} and 10^{-6}/s, respectively. The strength of the gouge increases with increasing temperature to 600°C, and the higher-temperature samples are also more likely to show stick-slip motion. Decreasing the sliding velocity by two orders of magnitude does not appreciably affect the strength of the gouge at a given temperature but it does increase both the tendency to stick-slip and the size of the stress drops.

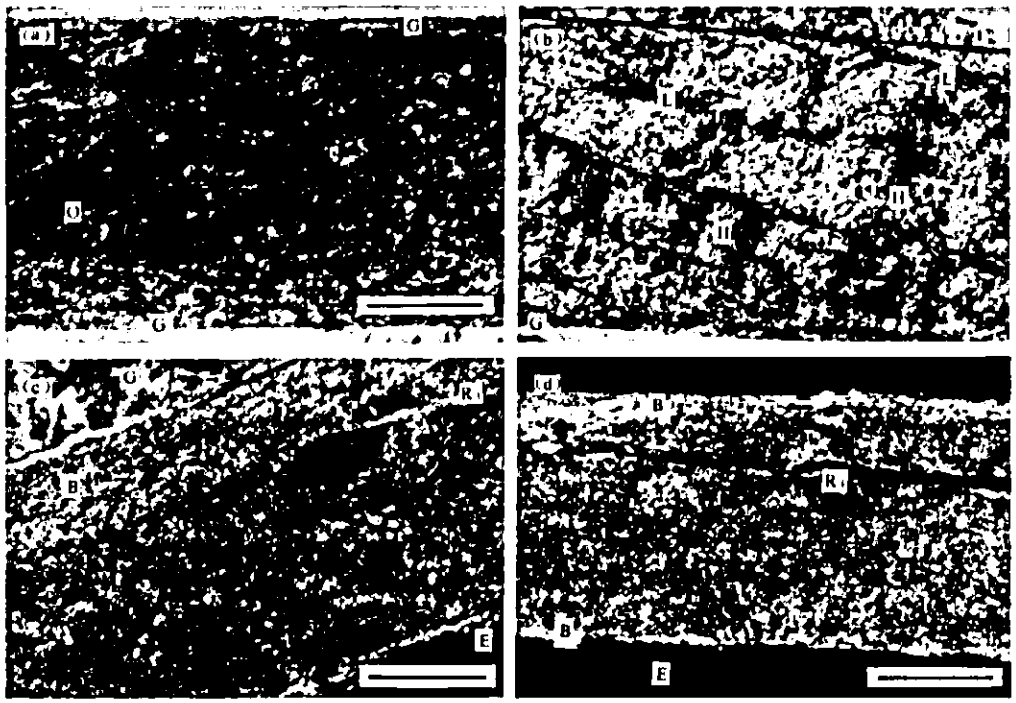

Fig. 3. Photomicrographs illustrating the range of textures observed in the illite gouge run products. The four samples are oriented to show right-lateral shear, and scale bars are all 0.2 mm in length. (a) Pervasively deformed gouge layer, shown in plane polarized light. The most obvious textural features in this view are the deformed opaque grains (O), whose long dimensions are oriented at 20°–30° to the boundary of the gouge layer with the granite cylinder (G) and extend upwards to the right. The clay minerals in this sample are oriented in roughly the same direction as the opaque grains. The clay fabric is bent by kink bands that are visible under crossed polarizers. (b) Incipient localization of shear. Crossed polarizers. Concentration of low-angle kink bands (L), at optical extinction, in narrow zones that crosscut the gouge layer and that form along the boundaries with the enclosing granite cylinder. High-angle kink bands (H), also at optical extinction, can be seen in the areas between these zones. (c) Well-developed, wide boundary (B) and narrower crosscutting (Riedel; R_1) shears. Crossed polarizers. Large, opaque-rich clast at upper right shows right-lateral offset along a Riedel shear. The clay fabric, deformed opaques, and kink bands are concentrated in the shears, and the rest of the gouge is only slightly deformed. E=epoxy, (d) Extreme localization of deformation to narrow boundary and Riedel shears, with rest of gouge completely undeformed. Crossed polarizers.

The boundaries between these shears and the remaining gouge are poorly defined, and the rest of the gouge layer still shows good development of a clay fabric, stretched grains, and kink/fold structures.

Well developed and relatively wide shear zones are seen in Fig. 3c. These shears have sharply defined boundaries with the adjoining illite gouge which are commonly marked by stretched opaque grains. All of the previously described deformation textures — clay fabric, kink bands, and stretched grains — become concentrated in the shears, and at least some of the gouge between the shears is relatively undeformed. In the extreme case of localized shear (Fig. 3d), all the deformation is concentrated in narrow boundary and crosscutting shears, and the rest of the gouge is completely undeformed. (The crosscutting shears that predominate in these experiments, with the orientation and sense of offset shown in Figs 3c and d, are generally referred to as Riedel shears.) Several of the 600°C samples that show this end-member texture contain some material that is isotropic under crossed polarizers and that has a pale lavender color in plane polarized light. The material occurs as one to three narrow, sub-parallel bands in the boundary shears. In some samples, an isotropic band crosses from one boundary shear to the other along a Riedel shear.

There is a close correlation between the deformation texture of a given sample and its sliding behavior, whatever the pressure-temperature-velocity conditions of the experiment. The samples with pervasive deformation (Figs 3a and b) slide stably, whereas the

samples with localized deformation (Figs 3c and d) show stick-slip motion if they also contain Riedel shears that make an angle greater than 14° with the boundary shears. If the maximum measured angles are less than 10°, the samples slide stably, and if the largest angles are between 10 and 14°, the samples show transitional behavior (e.g. 600°C, 4.8 μm/s sample in Fig. 2). The samples with the highest-angle Riedel shears (19–23°) generally have the largest stress drops.

QUARTZ AND GRANITE GOUGES

Run products from experiments using granite and quartz gouges have been examined to provide a comparison with the illite gouge. The granite gouge consists of Westerly granite which has been crushed and passed through a 0.090 mm sieve; it contains about 35% plagioclase and 25% each quartz and potash feldspar, with minor amounts of biotite, muscovite, opaques and other minerals (Moore *et al.*, 1983). The quartz gouge samples of Byerlee *et al.* (1978) with 9 mm or more shear displacement were reexamined for this study. The quartz gouge used in those experiments is a quartz sand of moderate roundness and sphericity and about 0.6 mm maximum grain diameter. Layers of granite gouge 0.25–4 mm in initial thickness were used in the experiments; the quartz gouge thicknesses were 2 and 4 mm. All of the experiments using quartz gouge were run at room temperature, whereas the experiments using the granite gouge were conducted at temperatures to 600°C.

Selected strength data for the granite gouge, which are representative of the behavior of both gouges at least at room temperature, are presented in Figs 4 and 5. Strength data for all the examined samples are contained in Summers and Byerlee (1977) and Moore *et al.* (1983, 1986b). The strengths of both the granite and quartz gouges increase with increasing effective pressure (Fig. 4). Both gouges slide stably at low pressures and show stick-slip motion at high pressures. Increasing the thickness of the gouge layer leads to a slight decrease in the size of the stress drops but does not affect the strength at a given set of experimental conditions (Summers and Byerlee, 1977; Byerlee *et al.*, 1978). Increasing the temperature to 600°C does not appreciably affect the strength or sliding behavior of the granite gouge (Fig. 5); decreasing the sliding velocity does increase the tendency to stick-slip motion, however.

Photomicrographs of 4 mm-thick quartz gouge and 0.65 mm-thick granite gouge run products are shown in Figs 6 and 7, respectively. The deformation textures developed in the two quartzofeldspathic gouges are somewhat different from those of the clay-rich gouges, as would be expected from the different types and sizes of grains present. The kink bands and kink/fold structures, which are a feature of the clay-rich gouges and

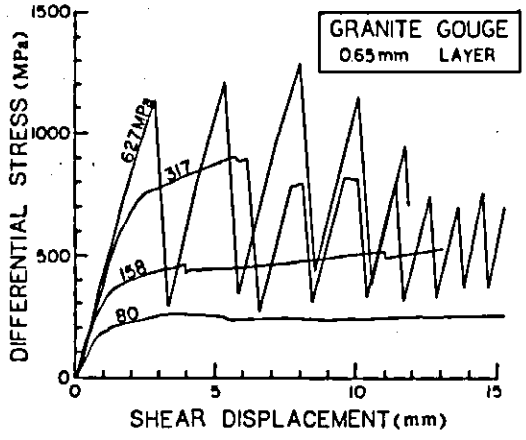

Fig. 4. Strength of granite gouge at confining pressures between 80 and 627 MPa, in experiments run dry at room temperature. The quartz gouge shows the same trends of increasing strength and a change from stable to stick-slip motion with increasing confining pressure.

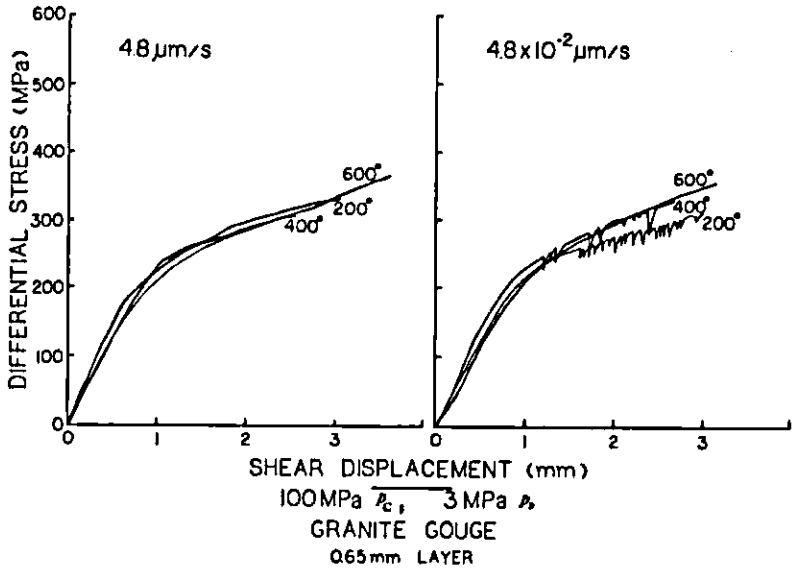

Fig. 5. Strength of heated granite gouge at 97 MPa effective pressure and sliding velocities along the sawcut of 4.8 and 4.8 × 10^2 μm/s, which correspond to strain rates of 10^{-4} and 10^{-6}/s, respectively. Unlike the illite-rich gouge (Fig. 2), the granite gouge shows no obvious changes in strength or sliding behavior with temperature increase to 600°C. Decreasing the sliding velocity does promote stick-slip motion in the granite gouge, however.

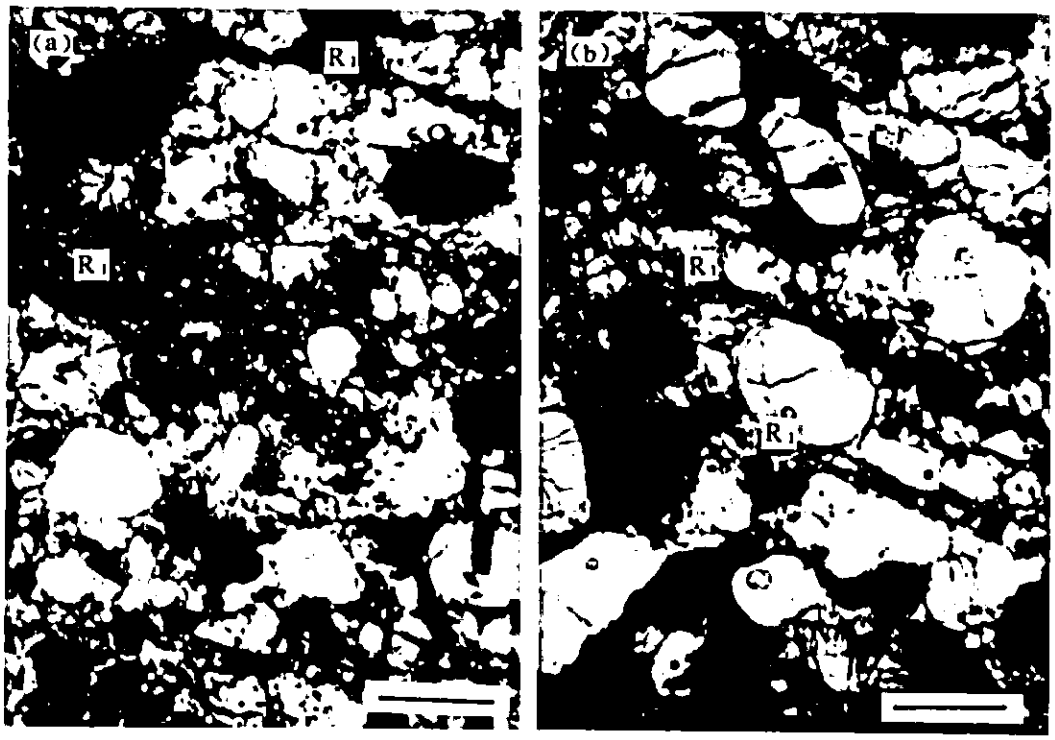

Fig. 6. Photomicrographs of (a) stably sliding (200 MPa *Pc*, dry, room temperature) and (b) stick-slip (470 MPa *Pc*, dry, room temperature) samples of quartz gouge of 4 mm initial width. The scale bars are 0.5 mm long; the lower half of the width of the gouge layer is shown in each photo. The shearing direction is right-lateral in both photographs. The average grain size of the stably sliding sample (a) is smaller than that of the stick-slip sample (b), and several of the quartz grains in (b) retain their original rounded shapes. The Riedel shears are wider and the measured Riedel angles are smaller in the stably sliding sample. Crossed polarizers; symbols as in Fig. 3.

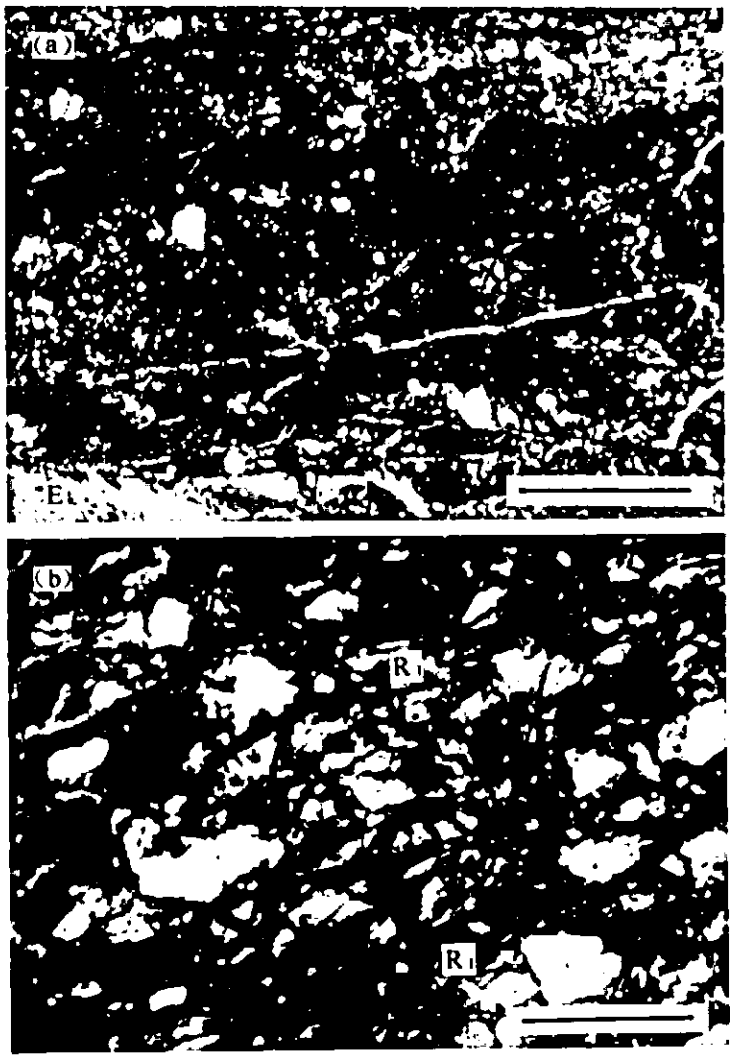

Fig. 7. Photomicrographs of (a) stably sliding (80 MPa *Pc*, dry, room temperature) and (b) stick-slip (627 MPa *Pc*, dry, room temperature) samples of granite gouge, of 0.65 mm initial thickness. Crossed polarizers; scale bars are 0.2 mm long. The shearing direction is left-lateral in both views. Grain size reduction is much more pronounced in these samples than in the 4 mm-thick samples shown in Fig. 6; however, the same textural variations relative to sliding behavior are observed at both thicknesses. Symbols as in Fig. 3.

which require a clay fabric to form, are not developed in the quartzofeldspathic samples. Instead, fracturing and crushing of the quartz and feldspar grains are prominent processes. Fracturing is concentrated at the points of contact between adjoining grains, and the cracks do not appear to have any preferred orientation. Crushed grains fill the spaces between intact grains, producing a compacted gouge of reduced porosity.

The granite and quartz gouge run products contain subsidiary shears similar to those found in the illite gouge; in these samples, however, the shears are zones of intense grain size reduction. Shear zone development and associated deformation in the quartzofeldspathic gouges show variations that are correlated with the sliding behavior of the samples. In the samples that slide stably, deformation is distributed across much of the gouge layer (Figs 6a and 7a). Shear zones are not well developed along the gouge-rock cylinder boundaries, although in the granite gouge opaque and mica grains right at the interface are smeared out. The samples do contain many Riedel shears, however, that are grouped into wide belts across the gouge layer. The gouge between the closely spaced Riedel shears in the belts shows a greater average grain size reduction than that found in the wider areas separating the belts, giving the gouge a crosswise layered appearance.

Stretched opaque and mica grains are found throughout the granite gouge, but the amount of elongation is greatest in the belts of Riedel shears. Individual Riedel shears in the granite gouge make angles up to 13° with the boundary of the gouge layer; angles in the quartz gouge are as high as 24°. Decreasing the thickness of the gouge layer (compare Figs 6a and 7a) leads to increases in the amount of grain size reduction and in the number of Riedel shears, but the orientations of the Riedel shears are unchanged.

In the samples that show stick-slip motion (Figs 6b and 7b), the boundary shears are better developed, the belts of Riedel shears are much narrower and spaced farther apart, and individual Riedel shears are more sharply defined and make higher angles with the boundary shears (20° maximum, granite gouge; 33° maximum, quartz gouge). The wide areas of gouge between the belts of Riedel shears do not show much grain size reduction, and opaque and mica grains in those areas are essentially undeformed. For a given layer thickness, therefore, the gouge has a coarser-grained appearance in the stick-slip samples than in the stably sliding ones. The boundary shears also contain one or more narrow, subparallel bands of the lavender-tinged isotropic material, and several of the Riedel shears contain single strands of isotropic material.

DISCUSSION

Comparison of Results

Petrographic examination of representative clayey and quartzofeldspathic gouges has shown that stick-slip motion in both types of gouge is correlated with (i) the localization of shear along subsidiary shear zones and (ii) an increase in the angle between the boundary and Riedel shears. Similiar relationships have also been described in some other studies. Moore *et al.* (1986b) noted a possible correlation between Riedel angles and sliding motion for granite, serpentine, and montmorillonite-rich gouges run at elevated temperatures and 3 MPa fluid pressure. Ma and Ma (1987) measured decreases in strength and a transition from stick-slip to stable motion with increasing temperature for quartz and calcite gouges. The transition to stable slip in their samples occurred between 400° and 500° for the quartz gouge and between 200° and 300°C for the calcite gouge. The 200°C quartz samples contained Riedel shears at angles of 18–25° to the boundary, whereas the 400° and 500°C run products yielded Riedel angles of 15–20°. Riedel angles of 20–25° were measured in the 200°C calcite samples, but the angles were only 10–15° in the 300–400°C calcite run products. Logan *et al.* (1979) also conducted experiments on heated calcite gouge. Their results are consistent with those of Ma and Ma (1987), although they reported slightly lower Riedel angles of 15–20° for their stick-slip samples and 8–10° for their stably sliding samples.

The results of this study and that of Ma and Ma (1987) indicate that, although the different gouge types show similar trends in Riedel angle relative to their sliding behavior, the actual size of the angles may be a function of their mineral contents. For example, the angles measured for the illite and granite gouges are comparable and consistently lower than those in the quartz gouge. Similarly, Logan *et al.* (1979) found that the Riedel angles measured in a pure quartz gouge were higher than those in a pure potash feldspar gouge, for samples run under comparable experimental conditions. The differences in reported Riedel angles between the samples of calcite gouge studied by Logan *et al.* (1979) and Ma and Ma (1987) may be caused by differences in initial grain size or composition of the calcite; alternatively, they may reflect differences in the measuring procedures used in the two studies.

Model

The observed correlations between deformation textures and sliding behavior can be explained as follows: For a sample showing pervasive deformation, if an obstruction develops in any one spot in the gouge layer, the shear can be taken up by the rest of the

gouge. In contrast, the localization of slip along narrow shear zones creates the potential for significant stress build-ups leading to stick-slip, if motion is impeded at some point along the shears. The high Riedel angles would provide the impediment to continuous slip by inhibiting stress transfers at the intersection between the boundary and Riedel shears. As observed in this study and also by Logan *et al.* (1979), localization of shear is a necessary but not a sufficient requirement for stick-slip motion; and the high intersection angles between Riedel and boundary shears may act as physical barriers. The higher the angle the greater the degree of obstruction to be expected, which is consistent with the correlation between the size of the stress drops and the Riedel angles in the illite gouge. The minimum angle for motion to be measurably impeded is a function of the mineralogy of the gouge.

The relative importance of the Riedel shears to the overall slip pattern has been debated (e.g. Engelder *et al.*, 1975; and Byerlee *et al.*, 1978). The experimental samples containing isotropic material support the suggestion that Riedel shears form part of the main slip path. Sketch maps of the isotropic bands in two of the illite run products are shown in Figs 8a and b. The isotropic material is either glass or extremely fine-grained gouge, and it is representative of concentrated slip. In both samples, an isotropic band switches from one side of the gouge layer to the other along a Riedel shear.

It is possible that the Ridel shear orientations are a result rather than the cause of the type of sliding motion. This question cannot be answered yet, because the controls on the Riedel shear orientations are not fully understood. Mandl *et al.* (1977) demonstrated experimentally that Riedel shears correspond to Coulomb shears; and if the deformation is of the simple shear type, as is generally assumed (e.g., Tchalenko, 1970; Logan *et al.*, 1979), the Riedel angle should equal one-half the angle of internal friction of the gouge material. For the heated illite gouge samples, however, the angle of internal friction obtained from the Riedel shear orientations differs from the value calculated from the plots of shear versus normal stress (Moore *et al.*, 1989). The assumption of simple shear may therefore be inappropriate for these samples or perhaps some additional factor affects the site of the Riedel angle.

Application to Fault Zones

The San Andreas and associated strike-slip faults in California contain both locked (stick-slip) and creeping (stable slip) sections along their lengths. In the locked portions of these faults, motion accompanying earthquakes is localized along subsidiary fractures

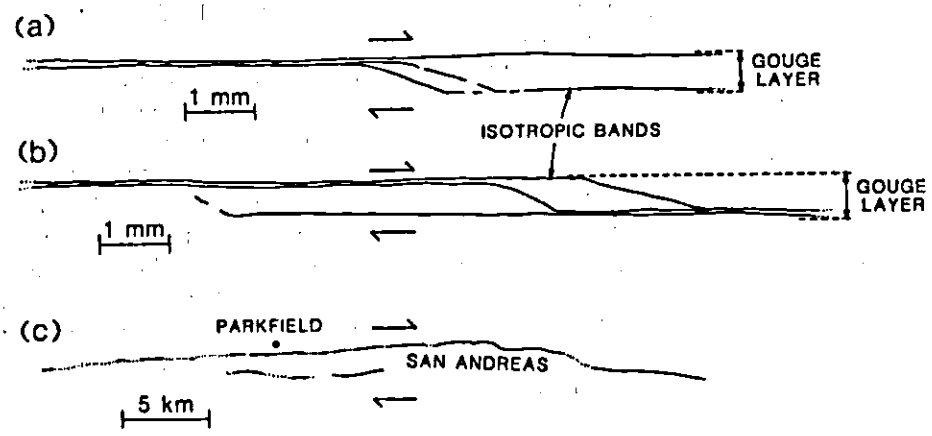

Fig. 8. (a–b) Sketch maps of isotropic bands found in the boundary and Riedel shears of 2 illite gouge run products. The isotropic material marks the lines of concentrated slip in the samples; some of the bands cross from one boundary of the gouge layer to the other along Riedel shears. (c) Maps of surface fractures accompanying the 1966 Parkfield earthquake on the San Andreas fault in central California, from Brown and Vedder (1967).

in a much wider fault zone (see Allen, 1981, and references contained therein). In addition, the fracture traces developed during recent earthquakes along the San Andreas commonly form *en echelon* patterns that have been correlated with the Riedel shears developed in laboratory experiments (Wallace, 1973). In creeping sections, motion may either be localized or distributed across the entire width of the fault (e.g. Radbruch, 1968). These field observations are generally consistent with the deformation textures in our experimental samples.

If the experimentally observed relationship between Riedel shear orientations and sliding behavior is also valid in natural faults, the orientation of recent fault traces in the locked sections of the San Andreas and associated faults should differ from those developed in the creeping sections. We plan to study the mapped traces of the San Andreas, to look for such differences. The work will focus on the *en echelon* structures described by Wallace (1973) and on sections of the fault similar to that shown in Fig. 8c, which shows the extent of fracturing associated with the 1966 Parkfield eartquake, taken from Brown and Vedder (1967). The fracture traces at Parkfield closely approximate the mapped isotropic bands in the experimental samples (Figs 8a and b). The geology at all points of interest along the fault must also be examined, because of the variations in Riedel shear orientations with the mineralogy of the fault gouge.

REFERENCES

ALLEN, C.R. (1981) The modern San Andreas fault. In: *The Geotectonic Development of California*, Rubey (W.G. ERNST, Ed.) **1**, 511–534. Prentice-Hall, Englewood Cliffs.

BROWN, R.D., Jr. and VEDDER, J.C. (1967) Surface tectonic fractures along the San Andreas Fault. *U.S.G.S. Prof. Paper*, 579, 2–23.

BYERLEE, J., MJACHKIN, V., SUMMERS, R. and VOEVODA, O. (1978) Structures developed in fault gouge during stable sliding and stick-slip. *Tectonophysics* **44**, 161–171.

DENG, Q. and ZHANG, P. (1984) Research on the geometry of shear fracture zones. *J. Geophysics Res.* **89**, 5699–5710.

DENG, Q., WU, D., ZHANG, P. and CHEN, S. (1986) Structure and deformational character of strike-slip fault zones. *Pure Appl. Geophys.* **124**, 203–223.

ENGELDER, J.T., LOGAN, J.M. and HANDIN, J. (1975) The sliding characteristics of sandstone on quartz fault gouge. *Pure Appl. Geophys.* **113**, 69–86.

LOGAN, J.M., FRIEDMAN, M., HIGGS, N., DENGO, C. and SHIMAMOTO, T. (1979) Experimental studies of simulated gouge and their application to studies of natural fault zones. *U.S.G.S. Open-File Rep.* 79–1239: 305–343.

MA SHENGLI AND MA JIN (1987) Experimental study on deformation fabrics of quartz and calcite in shear zone. *Seismol. Geol.* **9**(4), 1–18.

MANDL, G., DE JONG, L. N. J. and MALTHA, A. (1977) Shear zones in granular material. *Rock Mech.* **9**, 95–114.

MOORE, D.E., SUMMERS, R. and BYERLEE, J.D. (1983) Strengths of clay and non-clay fault gouge at elevated temperatures and pressures. *Proc. 24th U.S. Symp. Rock Mech.* 489–500.

MOORE, D.E., SUMMERS, R. and BYERLEE, J.D. (1986a) Strength measuements of heated illite gouge at low and high pore pressures. *U.S.G.S. Open-File Rep.* 86–578.

MOORE, D.E., SUMMERS, R. and BYERLEE, J. (1986b) The effect of sliding velocity on the frictional and physical properties of heated fault gouge. *Pure Appl. Geophys.* **124**, 31–52.

MOORE, D.E., SUMMERS, R. and BYERLEE, J.D. (1989). Sliding behavior and deformation textures of heated illite gouge. *J. Struct. Geol.* **11**, 329–342.

RADBRUCH, D.H. (1968) Discussion to paper by L. S. Cluff. In: *Proceedings of Conference on Geologic Problems of San Andreas Fault System* (W.R. DICKINSON and A. GRANTZ, Eds) *Stanford Univ. Publ. Geol. Sci.* **11**, 67.

SUMMERS, R. and BYERLEE, J. (1977) Summary of results of frictional sliding studies, at confining pressures up to 6.98 kb, in selected rock materials. *U.S.G.S. Open-File Rep.* 77–142.

TCHALENKO, J.S. (1970) Similarities between shear zones of different magnitudes. *Geol. Soc. Am. Bull.* **81**, 1625–1640.

WALLACE, R.E. (1973) Surface fracture patterns along the San Andreas Fault. In: *Proceedings of the Conference on Tectonic Problems of the San Andreas Fault System* (R.L. KOVACH and A. NUR, Eds) *Stanford Univ. Publ. Geol. Sci.* **13**, 248–250.